

QCD corrections to W^+W^- production through gluon fusion

Fabrizio Caola^a, Kirill Melnikov^b, Raoul Röntsch^b, Lorenzo Tancredi^b

^a*CERN Theory Division, CH-1211, Geneva 23, Switzerland*

^b*Institute for Theoretical Particle Physics, KIT, Karlsruhe, Germany*

Abstract

We compute the next-to-leading order (NLO) QCD corrections to the $gg \rightarrow W^+W^- \rightarrow l_1^+ \nu_{l_2} \bar{\nu}_2$ process, mediated by a massless quark loop, at the LHC. This process first contributes to the hadroproduction of W^+W^- at $\mathcal{O}(\alpha_s^2)$, but, nevertheless, has a sizable impact on the total production rate. We find that the NLO QCD corrections to the $gg \rightarrow W^+W^-$ process amount to $\mathcal{O}(50)\%$, and increase the NNLO QCD cross sections of $pp \rightarrow W^+W^-$ by approximately two percent, at both the 8 TeV and 13 TeV LHC. We also compute the NLO corrections to gluonic W^+W^- production within a fiducial volume used by the ATLAS collaboration in their 8 TeV measurement of the W^+W^- production rate and find that the QCD corrections are significantly smaller than in the inclusive case. While the current experimental uncertainties are still too large to make these differences relevant, the observed strong dependence of perturbative corrections on kinematic cuts underscores that extrapolation from a fiducial measurement to the total cross section is an extremely delicate matter, and calls for the direct comparison of fiducial volume measurements with corresponding theoretical computations.

Keywords: QCD, NLO computations, vector bosons, LHC

The production of electroweak di-bosons, $pp \rightarrow VV$, is amongst the most important processes studied at the LHC. The Higgs decay mode $H \rightarrow VV$ will be central to precision measurements of the Higgs quantum numbers and couplings during Run II [1–8]. This requires extremely good control over the large $pp \rightarrow VV$ background, including in the Higgs off-shell region [9], which can be exploited to constrain HVV couplings [10] or the Higgs width [11–13]. Additionally, di-boson production probes the nature of the electroweak interactions, allowing New Physics effects to be either discovered or constrained through studies of anomalous gauge couplings. Finally, di-boson production serves as an important testing ground for our understanding of QCD in a collider environment.

At leading order (LO), weak boson pair production $pp \rightarrow VV$ occurs only through the $q\bar{q}$ partonic channel. The next-to-leading order (NLO) QCD corrections to this process have been studied extensively in the past [14–22]; recently the next-to-next-to-leading order (NNLO) QCD corrections have also been computed [23–28]. At this order, the gg partonic channel starts contributing [29–34] and, thanks to a relatively large gluon flux at the LHC, its contribution can be expected to be large. This is exactly what happens: the gluon fusion process contributes 60% of the NNLO QCD corrections

in ZZ production, and 35% of the NNLO QCD corrections in W^+W^- production. Radiative corrections to the gluon fusion channel formally contribute at next-to-next-to-next-to-leading order ($N^3\text{LO}$) but are expected to be significant [35]. Indeed, we showed recently that NLO QCD corrections to $gg \rightarrow ZZ$ increase its contribution to $pp \rightarrow ZZ$ by almost a factor of two making them important for phenomenology of ZZ production [36]. Moreover, the magnitude of these corrections exceeds the scale variation uncertainty of the NNLO QCD result which is commonly used to estimate the residual uncertainty of the theory prediction. The aim of this Letter is to report the results of a similar calculation for $gg \rightarrow W^+W^-$.

Run I measurements of the W^+W^- cross section undertaken by both ATLAS [37] and CMS [38, 39] showed a discrepancy at the level of $\mathcal{O}(2 - 2.5)$ standard deviations compared to the Standard Model (SM) prediction. This deviation has been studied in the context of physics beyond the Standard Model (BSM) [40–45], but there has also been a concerted effort from the theory community to understand the source of this discrepancy in terms of QCD effects. This includes the calculation of the total W^+W^- cross section to NNLO in QCD [26], as well as the examination of ambiguities caused by an extrapolation from the fiducial region to the total cross section, either in the context of parton showers [46] or through resummations [47–49]. As a consequence of these efforts, the discrepancy seems to have been resolved without recourse to BSM

Email addresses: fabrizio.caola@cern.ch (Fabrizio Caola), kirill.melnikov@kit.edu (Kirill Melnikov), raoul.roentsch@kit.edu (Raoul Röntsch), lorenzo.tancredi@kit.edu (Lorenzo Tancredi)

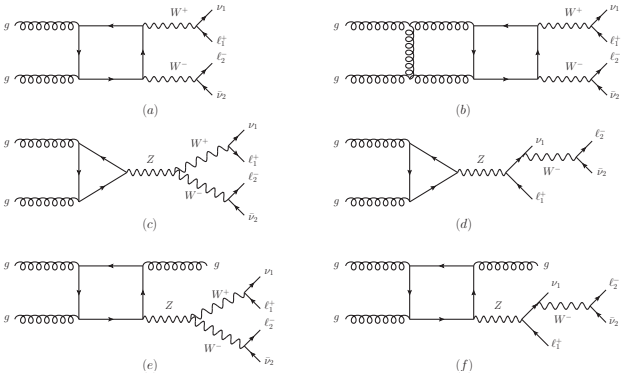


Figure 1: Representative Feynman diagrams that contribute to gluon fusion process $gg \rightarrow \nu_1 \ell_1^+ \ell_2^- \bar{\nu}_2$ through NLO in perturbative QCD.

effects, but these developments underlined the importance of comparing theoretical and experimental results for fiducial volume measurements, avoiding uncertainties related to the extrapolation. Motivated by these considerations, we also study the NLO QCD corrections to $gg \rightarrow W^+W^-$ in the fiducial region defined by the ATLAS cuts.

We begin by summarizing the technical details of the calculation, and refer the reader to Ref. [36] for a more extensive discussion. In Fig. 1 we present representative Feynman diagrams that are required for the calculation of the gluon fusion process $gg \rightarrow W^+W^-$ through NLO in perturbative QCD. The required two-loop contributions to $gg \rightarrow W^+W^-$ scattering amplitudes have been calculated in Refs. [50, 51]; we use the C++ code developed in Ref. [51] in our computation. We calculate the relevant one-loop real-emission amplitudes $gg \rightarrow W^+W^- + g$ using a combination of numerical [52] and analytic [53] unitarity methods. The virtual and real-emission contributions are combined using both the q_T [54] and the FKS [55] subtraction schemes, allowing for a check of the numerical stability of the final results and the consistency of the implementation in a numerical program.

Throughout the paper, we consider leptonic decays of the W -bosons, $gg \rightarrow W^+W^- \rightarrow \nu_1 \ell_1^+ \ell_2^- \bar{\nu}_2$. We note that if the leptons are of the same flavor and off-shell contributions are allowed then, strictly speaking, it is impossible to distinguish off-shell W^+W^- production from off-shell $ZZ \rightarrow \ell^+ \ell^- \nu \bar{\nu}$ production, so that both contributions need to be included. We do not consider this issue here and postpone its investigation to the near future.

We will now comment on the various contributions to $gg \rightarrow W^+W^-$ amplitudes. In addition to typical box-type amplitudes shown in Fig. 1(a), we need to consider amplitudes where gluons couple to Z^* and/or γ^* through the quark loop, see Figs. 1(c),(d). However, it was shown in Ref. [56] that the sum of these triangle diagrams vanishes to all loop orders for on-shell

colliding gluons. This implies that we only have to consider Z/γ^* -mediated amplitudes if an additional gluon is radiated, c.f. Figs. 1(e-f). Note that we also include the singly-resonant amplitudes in our calculation, see Fig. 1(f).

The most important difference with respect to our previous work is the treatment of the massive quark loops. In ZZ production, it is possible to separate the contribution of bottom and top loops, if one neglects the contribution of vector-axial triangle diagrams which are suppressed by the top mass. One can then consider gluon-initiated ZZ production through loops of five massless quark flavors. On the other hand, if W bosons are radiated from the quark loop, such a separation is obviously not possible since W -bosons mediate transitions within a given generation and mix the contributions of bottom and top quarks. Since we cannot compute two-loop diagrams with internal masses, for $gg \rightarrow W^+W^-$ amplitudes we neglect the contribution of the third generation entirely, and consider only massless quarks of the first two generations. However, for real-emission amplitudes which involve a Z/γ^* boson attached to the quark loop (Fig. 1(e) and (f)), we adopt our previous approach and also include massless bottom quarks in the loop. We expect that the accuracy of this approach is $\mathcal{O}(10\%)$; this estimate is based on the observation that the inclusion of the third generation in the computation of the $gg \rightarrow W^+W^-$ leading order cross section changes the result by approximately this amount [57, 58]. We have checked that the ratio of leading order cross sections $\sigma_{gg \rightarrow W^+W^-}^{3\text{gen}} / \sigma_{gg \rightarrow W^+W^-}^{2\text{gen}} \approx 1.1$ is practically independent of the collision energy and the kinematic cuts that we use later on to identify the fiducial volume cross section. This observation offers a simple way to account for the effect of the third generation: although we present the numerical results below omitting the contribution of the third generation, it can be included in an approximate way by increasing all our results by ten percent. This is the best one can do as long as the NLO QCD corrections to $gg \rightarrow W^+W^-$ process, mediated by a massive quark loop, remain unknown.

We now present the results for $gg \rightarrow W^+W^- \rightarrow \nu_e e^+ \mu^- \bar{\nu}_\mu$ cross sections. To perform the computation, we take the masses of the W and Z bosons to be $m_W = 80.398$ GeV and $m_Z = 91.1876$ GeV, their widths to be $\Gamma_W = 2.1054$ GeV and $\Gamma_Z = 2.4952$ GeV and the Fermi constant $G_F = 1.16639$ GeV⁻². We use $\mu = \mu_0 = m_W$ as the central value for the renormalization and factorization scale, and estimate the effect of the scale variation by calculating the cross section at $\mu = 2\mu_0$ and $\mu = \mu_0/2$. We use LO and NLO NNPDF3.0 parton distribution functions [59], accessed through LHAPDF6 [60] and one- and two-loop running of the strong coupling, for our LO and NLO results, respectively. We do not include the contribution from Higgs-mediated amplitudes. Unless stated otherwise,

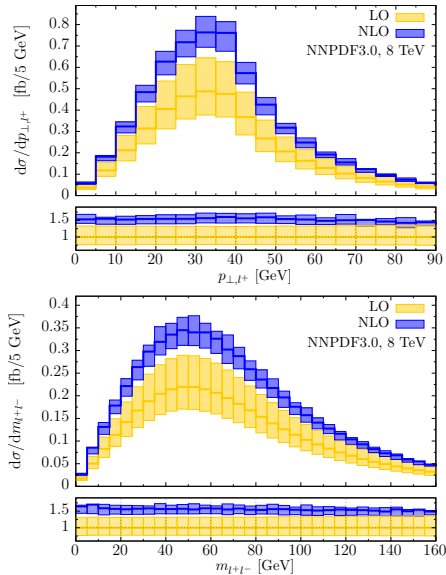


Figure 2: The transverse momentum of the positron p_{\perp,ℓ^+} (upper plot) and the invariant mass of the dilepton system $m_{\ell^+\ell^-}$ (lower plot) in $gg \rightarrow W^+W^- \rightarrow \nu_e e^+ \mu^- \bar{\nu}_\mu$ process at the $\sqrt{s} = 8$ TeV LHC. LO results are shown in yellow, NLO results are shown in blue. The central scale is $\mu = m_W$; the scale variation bands correspond to scale variations by a factor of two in either direction. The lower panes show the ratios of the LO and NLO distributions at each scale to the LO distribution at the central scale.

W bosons are produced on the mass shell. At $\sqrt{s} = 8$ TeV, we find the inclusive cross sections at LO and NLO to be

$$\sigma_{gg,LO}^{W^+W^-} = 20.9_{-4.8}^{+6.8} \text{ fb}, \quad \sigma_{gg,NLO}^{W^+W^-} = 32.2_{-3.1}^{+2.3} \text{ fb}, \quad (1)$$

where the superscript (subscript) refers to the value at $\mu = \mu_0/2$ ($\mu = 2\mu_0$). We note that the NLO QCD corrections increase the gluon fusion cross section by a factor of 1.24–1.80, with an increase by a factor of 1.54 for the central scale choice. This is similar to what was found in Ref. [36] for $gg \rightarrow ZZ$ production, when one takes into account the different choice made there for the central scale.

In order to put these results into context, we would like to estimate their impact on the NNLO QCD prediction for the $pp \rightarrow W^+W^-$ process at $\sqrt{s} = 8$ TeV presented recently in Ref. [26]. The results reported in Ref. [26] were obtained for stable W -bosons; to compare them with our results, we have to multiply them by the branching fractions for W decays into leptons. With the input parameters described above we find $\text{Br}(W \rightarrow \ell\nu_\ell) = 0.108$, in good agreement with experimental measurements. Then, taking the cross sections from Ref. [26] at $\mu = \mu_0$, we obtain

$$\sigma_{NLO} = 638.84 \text{ fb}; \quad \sigma_{NNLO+gg,LO} = 697.97 \text{ fb}. \quad (2)$$

It is stated in Ref. [26] that about 35% of the NNLO QCD corrections is due to the gluon fusion channel; this

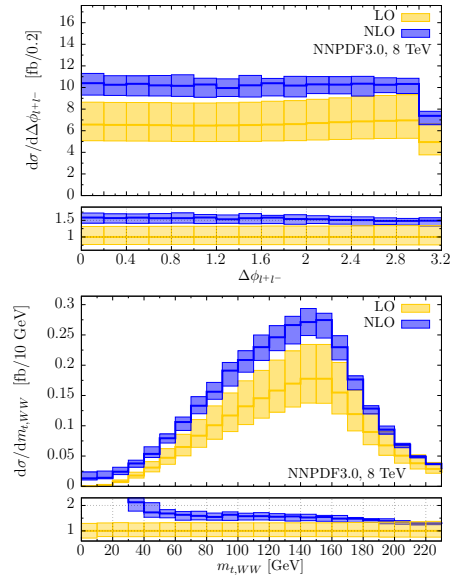


Figure 3: The azimuthal angle between the charged leptons $\Delta\phi_{\ell^+\ell^-}$ (upper plot), and the transverse mass of the W^+W^- system $m_{T,W}W$ (lower plot), in $gg \rightarrow W^+W^- \rightarrow \nu_e e^+ \mu^- \bar{\nu}_\mu$ process at the $\sqrt{s} = 8$ TeV LHC. LO results are shown in yellow, NLO results are shown in blue. The central scale is $\mu = m_W$; the scale variation bands correspond to scale variations by a factor of two in either direction. The lower panes show the ratios of the LO and NLO distributions at each scale to the LO distribution at the central scale.

implies that the $gg \rightarrow W^+W^- \rightarrow 2\ell 2\nu$ cross section used in Ref. [26] is $\mathcal{O}(21)$ fb which compares well with our result in Eq.(1). We now substitute the NLO QCD result for the gluon fusion cross section instead of the LO one and obtain¹

$$\sigma_{NNLO+gg,NLO} \approx 710 \text{ fb}. \quad (3)$$

Therefore, inclusion of the NLO corrections to the gluon-initiated partonic channel increases the total NNLO QCD cross section by about 2% percent. This shift is comparable to the residual theoretical uncertainty on the NNLO QCD prediction for $pp \rightarrow W^+W^-$, which is quoted as $\mathcal{O}(2\%)$ in Ref. [26]. We also note that the shift is much larger than the off-shell cross section for Higgs boson production $gg \rightarrow H^* \rightarrow W^+W^- \rightarrow 2\ell 2\nu$ which we estimate to be $\mathcal{O}(1)$ fb using the MCFM program [61].

We note that gluon fusion contributions both at leading and next-to-leading order are less important for $pp \rightarrow W^+W^-$ compared to $pp \rightarrow ZZ$. Indeed, in the latter case the corrections to the gluon fusion process were found to increase the NNLO corrections by approximately 50% [36] and move it beyond the estimated uncertainty of the NNLO result. The reason gluon fusion is more important for ZZ than for the W^+W^-

¹We note that including contributions of the third generation would increase this cross section by approximately 2 fb.

final state is a consequence of the fact that the quark initiated production cross section for $pp \rightarrow W^+W^-$ and the uncertainties of the final result are about a factor of seven larger than the quark initiated cross section for $pp \rightarrow ZZ$, while the gluon fusion contribution to W^+W^- process is only three times larger.

We repeat the calculation for proton-proton collisions at 13 TeV. For the $gg \rightarrow W^+W^- \rightarrow \nu_e e^+ \mu^- \bar{\nu}_\mu$ process, we find the LO and the NLO cross sections,

$$\sigma_{gg,\text{LO}}^{W^+W^-} = 56.5_{-11.5}^{+15.4} \text{ fb}, \quad \sigma_{gg,\text{NLO}}^{W^+W^-} = 79.5_{-5.9}^{+4.2} \text{ fb}. \quad (4)$$

The NLO corrections increase the cross section by a factor of 1.2 – 1.6, with an increase of 1.4 at the central scale. The relative size of QCD radiative corrections is, therefore, similar to that at 8 TeV. The consequences of this increase for the NNLO QCD prediction of $pp \rightarrow W^+W^-$ cross sections are again similar to what was described earlier for the 8 TeV case; the NLO QCD corrections to $gg \rightarrow W^+W^-$ increase the full NNLO cross section by about 2% which, roughly, corresponds to the scale uncertainty of the NNLO QCD computation [26].

Next, we discuss kinematic distributions. We present results for the 8 TeV LHC. We have also studied kinematic distributions at 13 TeV and found a qualitatively similar behavior. A representative sample for the 8 TeV LHC is shown in Figs. 2 and 3. In Fig. 2 we display the positron transverse momentum distribution p_{\perp,ℓ^+} and the distribution of the invariant mass of the dilepton system $m_{\ell^+\ell^-}$. In Fig. 3 we present the distribution of the azimuthal opening angle between the charged leptons $\Delta\phi_{\ell^+\ell^-}$ and the transverse mass of the W^+W^- system defined as

$$m_{T,WW} = \sqrt{2p_{\perp,\ell^+\ell^-} E_{\perp,\text{miss}} (1 - \cos \tilde{\phi})}. \quad (5)$$

In the definition of the transverse mass, we introduced the following notation: $p_{\perp,\ell^+\ell^-}$ is the transverse momentum of the $\ell^+\ell^-$ system, $E_{\perp,\text{miss}}$ is the missing energy, and $\tilde{\phi}$ is the azimuthal angle between the direction of the $\ell^+\ell^-$ system and the missing momentum. We observe that for all kinematic distributions shown in Figs. 2 and 3, with the exception of the $m_{T,WW}$ one, the NLO results can be obtained from the LO results by re-scaling the latter by the constant factor determined by the NLO QCD effects in the total cross section. The situation is different for the $m_{T,WW}$ distribution, where the LO distribution vanishes at low values of $m_{T,WW}$, leading to an infinite relative correction in this kinematic regime. This behavior is easily understood. Indeed, vanishing of $m_{T,WW}$ requires all leptons in the final state to be collinear. This is not possible at LO but may occur at NLO when the W^+W^- system as a whole recoils against an additional jet in the final state.² We also note that, with the exception of the last

	$\sigma_{\mu\mu,8 \text{ TeV}}$	$\sigma_{ee,8 \text{ TeV}}$	$\sigma_{e\mu,8 \text{ TeV}}$
$\sigma_{gg,\text{LO}}$ [fb]	$5.94_{-1.35}^{+1.89}$	$5.40_{-1.23}^{+1.71}$	$9.79_{-2.24}^{+3.13}$
$\sigma_{gg,\text{NLO}}$ [fb]	$7.01_{-0.17}^{-0.36}$	$6.40_{-0.16}^{-0.32}$	$11.78_{-0.34}^{-0.46}$

Table 1: LO and NLO gluon-initiated fiducial cross sections for in the ee , $\mu\mu$, and $e\mu$ decay channels. The kinematic cuts are defined in Ref. [62]. The central value corresponds to $\mu = \mu_0$; the upper (lower) value to $\mu = 0.5\mu_0$ ($2\mu_0$), respectively. We remind the reader that these numbers do not include contributions from the third generation, see text for details.

bin, the $\Delta\phi_{\ell^+\ell^-}$ distribution is remarkably uniform at LO, and this uniformity is maintained at NLO. This is an interesting feature since the Higgs-mediated process $gg \rightarrow H^* \rightarrow W^+W^- \rightarrow 2l2\nu$ produces a larger number of charged lepton pairs with a small relative opening angle $\Delta\phi_{\ell^+\ell^-}$.

We now turn to the discussion of the fiducial cross sections defined by a set of cuts used by the ATLAS collaboration [62] for measurements with ee , $\mu\mu$, and $e\mu + \mu e$ final states. These cuts are displayed in a concise way in Table 1 of Ref. [46] and we do not repeat them here. However, we note that these cuts include a veto on events with jets with the transverse momentum that exceeds 25 GeV. This is an important cut since it reduces the amount of real radiation at NLO and, therefore, is expected to reduce the magnitude of radiative corrections compared to the inclusive cross section case.

In Table 1, we present the fiducial volume cross sections for the gluon-initiated process at LO and NLO QCD in these three channels. In order to accurately account for the cuts, these results are computed allowing the W -bosons to be off the mass shell. The NLO QCD values for fiducial cross sections appear to be maximal at the central scale. For our choice of the central scale, the NLO corrections increase the fiducial cross sections by 18% – 20%, independent of the decay channel. This is substantially smaller than the relative size of radiative corrections found for the inclusive cross section. As already mentioned, this large difference between corrections to inclusive and fiducial volume cross sections is explained by the presence of a jet veto in the ATLAS cuts which removes real-emission contributions with a hard gluon. Since the hard gluon radiative cross section is positive, the NLO cross section with a jet veto is smaller than the cross section without it. A similar effect is known in Higgs production in gluon fusion [63].

Our observation of smaller radiative corrections in the fiducial volume cross section is important since it points towards potential problems with extrapolating fiducial volume cross sections to their inclusive values.

state; therefore, this effect should be seen in $q\bar{q} \rightarrow W^+W^-$ at NLO, if no cuts are placed on the leptons. We have checked that this is indeed the case using the program MFCM [61].

² This interpretation is of course independent of the initial

In the case of $gg \rightarrow VV$ such extrapolations completely ignore all the subtleties related to the gluon fusion channel since NLO QCD corrections to this mechanism of vector boson production are not included in Monte Carlo event generators. Matching our computation to existing NLO parton shower event generators is then desirable. While this may be challenging technically since the LO process is loop-induced, it does not require any conceptual modification of existing techniques to combine fixed order computations and parton showers.

We would like to examine the effects of the NLO corrections to the gg channel shown in Table 1 on the existing theoretical calculations of the fiducial cross sections. We compute these fiducial cross sections using MCFM [61] and the cuts from Ref. [46]. Included in this calculation are the $q\bar{q}$ contributions³ at NLO QCD, the Higgs production $pp \rightarrow H \rightarrow W^+W^-$ at NLO QCD and the LO gg contributions through quark loops of all flavors, with the top mass taken as $m_t = 172.5$ GeV and the Higgs signal/background interference at LO QCD. We then replace the LO massless gg cross sections in the fiducial volume with the corresponding NLO values. The 8 TeV cross sections (in fb) for the $\mu\mu$, ee and $e\mu + \mu e$ decay channels become⁴

$$\sigma_{\mu\mu, ee, e\mu+\mu e}^{q\bar{q}+H+gg, \text{NLO}} = (72.0_{-2.1}^{+1.3}, 66.3_{-1.7}^{+1.2}, 337.3_{-4.5}^{+6.3}). \quad (6)$$

Theoretical results in Eq.(6) should be compared with results of the ATLAS 8 TeV measurement

$$\sigma_{\mu\mu, ee, e\mu+\mu e} = (74.4_{-7.1}^{+8.1}, 68.5_{-8.0}^{+9.0}, 377.8_{-25.6}^{+28.4}), \quad (7)$$

where we combined statistical, systematic and luminosity uncertainties in quadratures. We see that the electron and muon channels agree perfectly whereas the central value of the $e\mu + \mu e$ channel differs by about 1.5 standard deviations. However, this picture is somewhat misleading, since we have not included the NNLO QCD corrections to the $q\bar{q}$ channel in the theory predictions in Eq.(6). While these corrections are unknown in the fiducial region, it is perhaps interesting to see what happens if one estimates them by re-scaling NNLO QCD corrections to the inclusive cross section by the ratio of fiducial and inclusive cross sections. In this case we find that the missing NNLO QCD corrections can increase the cross sections in Eq.(6) by $\mathcal{O}(4 - 20)$ fb for $ee(\mu\mu)$ and $e\mu + \mu e$ channels, respectively. Such an increase would make the theory prediction and experimental results agree to within one standard deviation for each of the three channels.

³Although we consistently talk about $q\bar{q}$ contributions, the qq initiated processes are, of course, included, following the standard routine of perturbative QCD computations.

⁴The NLO $q\bar{q}$ and LO gg results have opposite scale dependence, so their naive combination would lead to an accidentally small scale variation uncertainty. If the gg channel is included at NLO, the total uncertainty is dominated by the $q\bar{q}$ channel so a precise procedure of how to combine the $q\bar{q}$ and gg uncertainties is not important.

In summary We have calculated the NLO QCD corrections to the $gg \rightarrow W^+W^- \rightarrow l_1^+ \nu_1 l_2^- \bar{\nu}_2$ process at the LHC. These corrections increase the gluon fusion cross section by 20%–80%, depending on the center-of-mass energy and the scale choice. The impact of these corrections on the $pp \rightarrow W^+W^-$ production cross section is moderate; they increase the NNLO QCD theory prediction by about two percent, which is comparable to the current estimate of the theoretical uncertainty at NNLO. We have also calculated the $gg \rightarrow W^+W^-$ cross section through NLO in perturbative QCD subject to kinematic cuts used by the ATLAS collaboration to measure the $pp \rightarrow W^+W^-$ cross section. For the fiducial cross section, we found a smaller increase of around 20% for our central scale choice. Nevertheless, this contribution further increases the fiducial volume cross section, moving the theoretical result closer to the experimental one.

Acknowledgments We are grateful to S. Pozzorini and, especially, to J. Lindert for their help in checking the $gg \rightarrow W^+W^- + g$ scattering amplitude computed in this paper against the implementation in OpenLoops [64, 65]. We would like to thank P. Monni and G. Zanderighi for discussions on the fiducial measurements and for providing their implementation of the ATLAS experimental cuts. The research reported in this paper is partially supported by BMBF grant 05H15VKCCA. F.C. and K.M. thank the Mainz Institute for Theoretical Physics (MITP) for hospitality and partial support during the program *Higher Orders and Jets for LHC*.

References

- [1] G. Aad, et al., Phys. Rev. D91 (1) (2015) 012006.
- [2] G. Aad, et al., Eur. Phys. J. C75 (7) (2015) 335.
- [3] G. Aad, et al., Eur. Phys. J. C75 (5) (2015) 231.
- [4] G. Aad, et al., ATLAS Collaboration, arXiv:1508.02507.
- [5] V. Khachatryan, et al., Eur. Phys. J. C75 (5) (2015) 212.
- [6] V. Khachatryan, et al., Phys. Rev. D92 (1) (2015) 012004.
- [7] V. Khachatryan, et al., Phys. Lett. B736 (2014) 64.
- [8] V. Khachatryan, et al., Phys. Rev. D92 (7) (2015) 072010.
- [9] N. Kauer, G. Passarino, JHEP 08 (2012) 116.
- [10] A. Azatov, C. Grojean, A. Paul, E. Salvioni, Zh. Eksp. Teor. Fiz. 147 (2015) 410–425, [J. Exp. Theor. Phys.120,354(2015)].
- [11] F. Caola, K. Melnikov, Phys. Rev. D88 (2013) 054024.
- [12] J. M. Campbell, R. K. Ellis, C. Williams, JHEP 04 (2014) 060.
- [13] J. M. Campbell, R. K. Ellis, C. Williams, Phys. Rev. D89 (5) (2014) 053011.
- [14] B. Mele, P. Nason, G. Ridolfi, Nucl. Phys. B357 (1991) 409.
- [15] J. Ohnemus, J. F. Owens, Phys. Rev. D43 (1991) 3626–3639.
- [16] J. Ohnemus, Phys. Rev. D44 (1991) 1403.
- [17] S. Frixione, Nucl. Phys. B410 (1993) 280.
- [18] J. Ohnemus, Phys. Rev. D 50 (1994), 1931.
- [19] L. J. Dixon, Z. Kunszt, A. Signer, Nucl. Phys. B531 (1998) 3.
- [20] J. M. Campbell, R. K. Ellis, Phys. Rev. D60 (1999) 113006.
- [21] L. Dixon, Z. Kunszt, A. Signer, Phys. Rev. D 60 (1999), 114037.
- [22] J. M. Campbell, R. K. Ellis, C. Williams, JHEP 07 (2011) 018.

- [23] S. Catani, L. Cieri, D. de Florian, G. Ferrera, M. Grazzini, Phys. Rev. Lett. 108 (2012) 072001.
- [24] M. Grazzini, S. Kallweit, D. Rathlev, A. Torre, Phys. Lett. B731 (2014) 204.
- [25] F. Cascioli, T. Gehrmann, M. Grazzini, S. Kallweit, P. Maierhofer, A. von Manteuffel, S. Pozzorini, D. Rathlev, L. Tancredi, E. Weihs, Phys. Lett. B735 (2014) 311.
- [26] T. Gehrmann, M. Grazzini, S. Kallweit, P. Maierhofer, A. von Manteuffel, S. Pozzorini, D. Rathlev, L. Tancredi, Phys. Rev. Lett. 113 (21) (2014) 212001.
- [27] M. Grazzini, S. Kallweit, D. Rathlev, JHEP 07 (2015) 085.
- [28] M. Grazzini, S. Kallweit, D. Rathlev, Phys. Lett. B750 (2015) 407.
- [29] D. A. Dicus, C. Kao and W. W. Repko, Phys. Rev. D 36 (1987), 1570.
- [30] E. W. N. Glover and J. J. van der Bij, Nucl. Phys. B 321, (1989) 561.
- [31] E. W. N. Glover and J. J. van der Bij, Phys. Lett. B 219, (1989) 488.
- [32] T. Binoth, M. Ciccolini, N. Kauer, M. Kramer, JHEP 0503 (2005), 065.
- [33] T. Binoth, M. Ciccolini, N. Kauer and M. Kramer, JHEP 0612, (2006) 046 .
- [34] T. Binoth, N. Kauer, P. Mertsch, arXiv:0807.0024.
- [35] M. Bonvini, F. Caola, S. Forte, K. Melnikov, G. Ridolfi, Phys. Rev. D88 (3) (2013) 034032.
- [36] F. Caola, K. Melnikov, R. Röntsch, L. Tancredi, arXiv:1509.06734.
- [37] G. Aad, et al., Phys. Rev. D87 (11) (2013) 112001, [Erratum: Phys. Rev.D88,no.7,079906(2013)].
- [38] S. Chatrchyan, et al., Phys. Lett. B699 (2011) 25.
- [39] S. Chatrchyan, Phys. Lett. B721 (2013) 190.
- [40] D. Curtin, P. Jaiswal, P. Meade, Phys. Rev. D87 (3) (2013) 031701.
- [41] D. Curtin, P. Jaiswal, P. Meade, P.-J. Tien, JHEP 08 (2013) 068.
- [42] K. Rolbiecki, K. Sakurai, JHEP 09 (2013) 004.
- [43] P. Jaiswal, K. Kopp, T. Okui, Phys. Rev. D87 (11) (2013) 115017.
- [44] D. Curtin, P. Meade, P.-J. Tien, Phys. Rev. D90 (11) (2014) 115012.
- [45] J. S. Kim, K. Rolbiecki, K. Sakurai, J. Tattersall, JHEP 12 (2014) 010.
- [46] P. F. Monni, G. Zanderighi, JHEP 05 (2015) 013.
- [47] P. Meade, H. Ramani, M. Zeng, Phys. Rev. D90 (11) (2014) 114006.
- [48] P. Jaiswal, T. Okui, Phys. Rev. D90 (7) (2014) 073009.
- [49] P. Jaiswal, P. Meade, H. Ramani, arXiv:1509.07118.
- [50] F. Caola, J. M. Henn, K. Melnikov, A. V. Smirnov, V. A. Smirnov, JHEP 06 (2015) 129.
- [51] A. von Manteuffel, L. Tancredi, JHEP 06 (2015) 197.
- [52] R. K. Ellis, W. T. Giele, Z. Kunszt, JHEP 03 (2008) 003.
- [53] S. D. Badger, JHEP 01 (2009) 049.
- [54] S. Catani, M. Grazzini, Phys. Rev. Lett. 98 (2007) 222002.
- [55] S. Frixione, Z. Kunszt, A. Signer, Nucl. Phys. B467 (1996) 399.
- [56] J. M. Campbell, R. K. Ellis, G. Zanderighi, JHEP 12 (2007) 056.
- [57] J. M. Campbell, R. K. Ellis, C. Williams, JHEP 10 (2011) 005.
- [58] N. Kauer, JHEP 1312 (2013) 082.
- [59] R. D. Ball, et al., JHEP 04 (2015) 040.
- [60] A. Buckley, J. Ferrando, S. Lloyd, K. Nordström, B. Page, M. Rüfenacht, M. Schönherr and G. Watt, Eur. Phys. J. C 75 (2015) 3, 132.
- [61] J. Campbell, R.K. Ellis, C. Williams, <http://mcfm.fnal.gov>.
- [62] ATLAS collaboration, Tech. Rep. ATLAS-CONF-2014-033, CERN, Geneva (Jul 2014).
- [63] S. Catani, D. de Florian, M. Grazzini, JHEP 01 (2002) 015.
- [64] F. Cascioli, P. Maierhofer, S. Pozzorini, Phys. Rev. Lett. 108 (2012) 111601.
- [65] F. Cascioli, J. Lindert, P. Maierhöfer, S. Pozzorini, <http://openloops.hepforge.org>.